



Regolith Weathering and Sorption Influences Molybdenum, Vanadium, and Chromium Export via Stream Water at Four Granitoid Critical Zone Observatories

Justin B. Richardson^{1,2*} and Elizabeth K. King³

¹ Department of Geosciences, University of Massachusetts Amherst, Amherst, MA, United States, ² Earth and Atmospheric Sciences, College of Agriculture and Life Sciences, Cornell University, Ithaca, NY, United States, ³ Department of Earth, Ocean, and Atmospheric Sciences, University of British Columbia, Vancouver, BC, Canada

OPEN ACCESS

Edited by:

Julia Perdrial,
University of Vermont, United States

Reviewed by:

Angelica Vazquez-Ortega,
Bowling Green State University,
United States

Dragos George Zaharescu,
Georgia Institute of Technology,
United States

*Correspondence:

Justin B. Richardson
Soilbiogeochemist@gmail.com

Specialty section:

This article was submitted to
Biogeoscience,
a section of the journal
Frontiers in Earth Science

Received: 20 June 2018

Accepted: 19 October 2018

Published: 09 November 2018

Citation:

Richardson JB and King EK
(2018) Regolith Weathering
and Sorption Influences Molybdenum,
Vanadium, and Chromium Export via
Stream Water at Four Granitoid
Critical Zone Observatories.
Front. Earth Sci. 6:193.
doi: 10.3389/feart.2018.00193

Understanding the fate of oxyanions in the Critical Zone is important because of their biological significance and the potential for their use as geochemical tracers in terrestrial environments and subsurface systems. This study assessed the partitioning and transport of a suite of oxyanion metals (Mo, V, and Cr) in regolith profiles and stream waters from four granitoid Critical Zone Observatories (CZO) (Boulder Creek, Calhoun, Luquillo, and Southern Sierra). For regolith profiles, we compared Mo, V, and Cr in total digestions and two extractions targeting oxyanions adsorbed to organic matter and amorphous oxides ($\text{H}_2\text{O}_2 + 0.1 \text{ M}$ acetic acid) and secondary Fe oxides (citrate–bicarbonate–dithionite). Total Mo, V, and Cr ranged from 0.4 to 2.5 mg kg^{-1} , 16 to 208 mg kg^{-1} , and 0.2 to 55 mg kg^{-1} , respectively. The greatest concentrations of the oxyanions did not occur in surface soil samples, nor deepest regolith samples (7–10 m in depth), but instead in subsurface peaks that corresponded with secondary Fe oxides and total organic carbon. The average organic and amorphous oxide bound phase was 0.1–3.5% while the secondary Fe oxide fraction was 4–27% of the respective total concentrations for oxyanions, suggesting that secondary Fe oxides were an important phase across the regolith profile. Stream water Mo, V, and Cr concentrations ranged from 0.02 to 0.25 $\mu\text{g L}^{-1}$, 0.2 to 1.8 $\mu\text{g L}^{-1}$, and 0.08 to 0.44 $\mu\text{g L}^{-1}$, respectively. Our results demonstrate that the deep regolith (2–7 m in depth) play an active role in both sourcing and retention of oxyanions. In addition, we observed that increased weathering intensity at warmer, wetter climates does not always lead to increased depletion in regolith or stream water export, which implies the importance of transport processes within regolith. Further quantification of oxyanion export from regolith can aid in developing their use as geochemical tools for global weathering.

Keywords: deep regolith, oxyanions, stream export, Critical Zone, weathering profile, soil biogeochemistry

INTRODUCTION

The Critical Zone (CZ) is the thin region on Earth's surface where the atmosphere, hydrosphere, lithosphere, and biosphere interact through chemical, biological, and physical processes (e.g., Brantley et al., 2007; Chorover et al., 2007; Giardino and Houser, 2015). Exploring the natural processes that govern the CZ is important as they ultimately sustain terrestrial life and exert controls on the biotic and abiotic cycling of energy and nutrients (Amundson et al., 2007). However, the CZ exhibits substantial variations in climate, lithology, and biogeography, both across landscapes and with depth. It is paramount to understand and quantify the mechanisms, particularly the poorly understood processes occurring at depth, that influence the CZ's development and function (Brantley and Lebedeva, 2011; Giardino and Houser, 2015).

The biological importance of oxyanion metals is twofold as they can serve as micronutrients in a number of life-sustaining processes, but may also have toxic effects on organisms at elevated concentrations. For example, plant growth can be negatively impacted by total V concentrations greater than 0.8 mg L⁻¹ in soil solution (Larsson et al., 2013) and total Cr water concentrations greater than 5 mg L⁻¹ is considered hazardous to plants and animals (Singh et al., 2013). In this study, we investigate how lithology and climate influence the retention of oxyanions in the regolith and mobilization to stream water. We focus on molybdenum (Mo), chromium (Cr), and vanadium (V) because of their role as essential micronutrients and potential toxicity for organisms.

In addition to toxicity, the unique geochemistry and speciation patterns of oxyanions allows them to be proxies for various environmental parameters, particularly oxidation-reduction reactions and weathering. Molybdenum is a key component for a number of enzymatic processes that occur during nitrogen and sulfur metabolism and is also responsible for the biosynthesis of plant hormones (Kaiser et al., 2005). Of particular interest, Mo is a cofactor for the nitrogenase enzyme required for nitrogen fixation and can become a limiting micronutrient in forest soils (e.g., Barron et al., 2008). Low concentrations of Mo are required by plants, with typical foliar values ranging between 0.03 and 1.61 mg kg⁻¹ (Adriano, 2001). At concentrations exceeding 100 ppm in soils Mo can become toxic for plants, and at concentrations exceeding 10 mg kg⁻¹ in vegetation humans and animals are susceptible to molybdenosis (Gupta, 1997; Adriano, 2001).

Vanadium (V) is another trace metal oxyanion that enhances plant growth and serves as a micronutrient for a variety of biological processes. At low concentrations (<2 mg kg⁻¹), V has been shown to enhance chlorophyll synthesis and nitrogen fixation in plant tissues; however, higher concentrations may cause chlorosis and stunted growth (Kabata-Pendias, 2011). Due to similarities in their ionic radii, V can substitute for Ca and Mg, inhibiting chlorophyll generation, protein production, ATP formation, cellular pH, and enzymatic activities at high abundance within plant tissues (Cantley et al., 1977, 1978; Marschner et al., 1986; Crans et al., 1995; Larsson et al., 2013). Nevertheless, V toxicity in plants are uncommon due to its

poor translocation from belowground to aerial tissues in plants (Adriano, 2001). There is no significant data to conclude that V is a necessary part of nutrition for humans (Imtiaz et al., 2015).

The biological importance of Cr is highly dependent on its oxidation state. Chromium(VI) does not serve any known roles for plants or animals, is a highly toxic carcinogen for humans (Kotaš and Stasicka, 2000; Dayan and Paine, 2001; Levina et al., 2003). Chromium (III), however, is essential for humans as it has been shown to be a cofactor for biologically active molecules that enhance the effects of insulin on target tissues; Cr(III) deficiencies include abnormal glucose utilization and increased insulin requirements (see Kotaš and Stasicka, 2000; Dayan and Paine, 2001). Chromium toxicity in plants is possible in very acidic soils with <5 pH, but is uncommon in soils with >5 pH due to low bioavailable concentrations (Adriano, 2001).

The retention and mobility of oxyanions (Mo, V, and Cr) are largely controlled by climate, weathering, and sorption reactions, all of which are variable in the Critical Zone. Molybdenum concentrations across all rock types range from 0.3 to 300 mg kg⁻¹ (Adriano, 2001), and all soil types range from 0.01 to 17 mg kg⁻¹ (Kabata-Pendias, 2011). Molybdenum exists in oxic soils primarily as the molybdate oxyanion (MoO₄²⁻, +VI oxidation state) with molybdic acid (H₂MoO₄) and its oxyanion (HMoO₄⁻) becoming increasingly present below pH 4, (Adriano, 2001; Alloway, 2013). Vanadium concentrations in rocks range from 20 to 250 mg kg⁻¹ while soils have a broader range of 3–500 mg kg⁻¹ depending on the initial concentration of their parent material (Adriano, 2001; Kabata-Pendias, 2011). Vanadium can be present as V(IV), mainly as VO₂ (vanadyl), whereas V(V) exists as the oxyanions H₂VO₄⁻¹ or as HVO₄⁻² (collectively referred to as vanadate), depending on the pH and oxidation status. Vanadate is considered the most toxic vanadium species (Martin and Kaplan, 1998; Larsson et al., 2013). Chromium concentrations in soils range from 2 to 150 mg kg⁻¹ and is found mainly in two oxidation states, the trivalent Cr(III) and the hexavalent Cr(VI) (Adriano, 2001).

The terrestrial geochemistry of Mo, V, and Cr is a function of sorption processes and chemical speciation. Under oxic conditions, Mo, V, and Cr oxyanion sorption onto soil solids is determined by Fe and Al oxides, clay minerals and organic matter, of which most are pH dependent (e.g., Gäbler et al., 2009; Pérez et al., 2014; Wisawapipat and Kretzschmar, 2017). As an example, adsorption of MoO₄²⁻ ions from soil solution onto positively charged metal oxides occurs between pH 4 and 5 (Riley et al., 1987; Gupta, 1997; Xu et al., 2013). In acidic soils, molybdate, vanadate, and chromate anions are sorbed onto positively charged Fe, Mn, and Al oxides as well as clay minerals and organic matter (Grove and Ellis, 1980; Pérez et al., 2014; King et al., 2016; Larsson et al., 2017; Wisawapipat and Kretzschmar, 2017). In addition, sorption to primary minerals such as inherited clay minerals like illite can also occur. In three Swedish soils, V(IV) was predominantly bound to primary minerals (Gäbler et al., 2009; Larsson et al., 2015; Wisawapipat and Kretzschmar, 2017). Oxyanion sorption to organic matter, Al and Fe oxides, and clay minerals in soils is important as it directly controls the retention and export of Mo, Cr, and V to stream waters (Kerr et al., 2008).

The influence of deep regolith—the unconsolidated layer of physically and chemically weathered rock that overlies unweathered bedrock—on oxyanion biogeochemistry in the Critical Zone is largely unconstrained below 2 m depth. Previous studies of Mo, Cr, and V sourcing to stream waters have primarily focused on surface soils <0.3 m depth (e.g., Salvador-Blanes et al., 2006; Gäbler et al., 2009; Wichard et al., 2009; Pérez et al., 2014; Morrison et al., 2015; Larsson et al., 2017; Wisawapipat and Kretzschmar, 2017) or only aqueous systems (e.g., Kerr et al., 2008; Gardner et al., 2017). However, regolith underlying soils at depths >1 m may be an important source of metals to surface waters and may also influence their immobilization. Here, we investigated the importance of regolith on oxyanion geochemistry at four Critical Zone Observatories (CZOs) developed on monolithic granitoid parent material, spanning a diverse climatic gradient (wet, hot tropical forest to cold, dry mountain-steppe). We hypothesized that CZOs with more secondary Fe oxide phases will have greater oxyanion sorption deeper within their profiles (>1 m depth) beyond the typical depth of surface soils (<0.3 m depth). Illuminating the role of the deep CZ is essential to capture its control on soil and surface water geochemistry.

MATERIALS AND METHODS

Critical Zone Observatories (CZOs)

Boulder Creek CZO

Boulder Creek CZO is located in Arapahoe National Forest at the front range of the Rocky Mountains in north central Colorado, (Figure 1). Regolith samples were collected by borehole drilling in June 2014 from Gordon Gulch, a valley with low topographic relief, within the Boulder Creek CZO. Eight regolith samples were collected over a 7.0 m depth profile with samples collected every 0.5 m for the top 2.5 m and one deep sample at 7.0 m. Gordon Gulch is characterized by a montane-steppe climate with a mean annual temperature (MAT) of 4°C and a mean annual precipitation (MAP) of 735 mm year⁻¹, with the majority of precipitation occurring between March and May (Table 1) (Dethier and Bove, 2011; Aguirre et al., 2017). The lithology of Gordon Gulch is dominated by biotite-gneiss (Dethier and Bove, 2011) and is forested with evergreen vegetation, primarily lodgepole pine (*Pinus contorta*)

and ponderosa pine (*Pinus ponderosa*) (Dethier and Bove, 2011; Barnes et al., 2012). Despite the low MAP, Boulder Creek CZO regolith is moderately weathered, on the basis of Ca, K depletion and presence of neoformed kaolinite (Condie et al., 1995; Dethier and Bove, 2011). Stream water samples were collected under baseflow conditions from the permanent flowing river in Gordon Gulch in March and April of 2017, using acid washed HDPE bottles following USGS water sampling techniques (United States Geological Survey [USGS], 2006).

Calhoun CZO

The Calhoun CZO is located in the Southern Piedmont in South Carolina (Figure 1), within the Calhoun Experimental Forest, and has been extensively studied to inform researchers about land and water degradation caused by agricultural uses (e.g., Richter and Markewitz, 2001). The sampling location at Calhoun CZO is on a low relief hill, derived from granitic-gneiss. The climate is subtropical with a MAT of 16°C and a MAP of 1,250 mm year⁻¹ (Table 1). Vegetation is dominated by loblolly pine (*Pinus taeda*), mixed hardwoods (primarily oak, *Quercus* spp.), and hickory (*Carya* spp.) (Richter and Markewitz, 2001). This study focused on samples collected every 0.6 m within a 7.6 m weathering profile collected from Research Area 1. Details of the collection and processing of drill core samples can be found in Bacon et al. (2012). In brief, soil samples (0–6.0 m) were collected from three cores while regolith was sampled with a three-wing auger bit (6.1–18.3 m). Samples were crushed, sieved to <2 mm, and air-dried. Bacon et al. (2012) has noted regolith at Calhoun CZO is intensively weathered, on the basis of Ca, K depletion in the upper 10 m. Stream water samples were collected under baseflow conditions from the nearest flowing surface water source, Watershed 4 stream, in March and April, 2017 using acid washed HDPE bottles following USGS water sampling techniques (United States Geological Survey [USGS], 2006).

Luquillo CZO

The Luquillo CZO is located in the El Yunque National Forest in northeastern Puerto Rico (Figure 1), and has also been studied as a Long-Term Ecological Research site and a USGS Water, Energy, and Biogeochemical Budgets (WEBB) site. The Luquillo CZO is a tropical montane forest and has a MAT of 21°C (Murphy et al., 2012). Precipitation increases with elevation from 2,500 to 4,500 mm year⁻¹ (Garcia-Martino et al., 1996). This paper focuses on the Guaba study site, a montane ridge that receives a MAP of 4,200 mm year⁻¹ and is located 680 m.a.s.l. in the Rio Icacos watershed (Table 1) (Murphy et al., 2017). The most abundant tropical vegetation at the Guaba study site were *Dacryodes excelsa*, *Prestoea montana*, *Sloanea berteriana*, *Cordia borinquensis*, *Manilkara bidentata*, *Schefflera morototoni*, *Cecropia schreberiana*, *Micropholis garciniifolia*, *Henriettea squamulosa*, and *Quararibea turbinata* (Weaver and Gould, 2013). Surface soil (top 0.3 m of regolith) and upper regolith samples were collected in 2017 down to 1.8 m depth. Deeper regolith samples were subsampled in 2010 from archived material from site LG1 (Buss et al., 2005, 2017) and borehole LGW1 (Buss and White, 2012; Orlando et al., 2016). In total, eleven regolith samples were analyzed. Samples were spaced

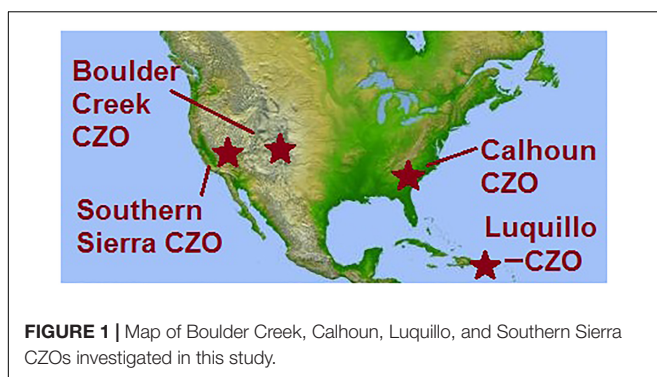


TABLE 1 | Climate, ecosystem, and geologic properties of sampling sites for the four Critical Zone Observatories (CZO).

Study area		Mean elevation m.a.s.l	Latitude	Longitude	MAT °C	MAP mm year ⁻¹	Vegetation	Soil	Bedrock
Boulder Creek CZO	Gordon gulch watershed	2,716	40° 01' 09" N	105° 28' 39" W	4	735	Evergreen forest	Inceptisols	Granite-gneiss
Calhoun CZO	Research Area 1 – Watershed 1	124	34° 36' 23.6" N	81° 43' 24.8" W	16	1,250	Pine-hardwood	Ultisols	Granitic gneiss
Luquillo CZO	Rio Icacos watershed	680	18° 17' 02" N	65° 47' 20" W	21	4,200	Tropical forest	Inceptisols	Quartz diorite
Southern Sierra CZO	Providence Creek – P301	1,250	37° 03' 36" N	119° 11' 27" W	9	1,100	Coniferous	Inceptisols	Granodiorite

every 0.4 m down to 1.8 m depth, with three deeper samples collected at 3.1 m, 4.2 m, and 8.6 m depth. An intact regolith sample was collected from 1.8 m depth, at the surface soil-regolith interface. Regolith at Luquillo CZO is intensively weathered, on the basis of Fe and base cation depletion throughout the upper 6 m (Buss et al., 2005, 2017). Stream water samples were collected under baseflow conditions (White et al., 1998; Pett-Ridge et al., 2009) from the Rio Icacos in February and March of 2017 using acid washed HDPE bottles following USGS water sampling techniques (United States Geological Survey [USGS], 2006).

Southern Sierra CZO

The Southern Sierra CZO is located in Fresno County, California (Figure 1), within the Kings River Experimental Watershed (KREW), a long-term research site established by the Pacific Southwest Research Station of the United States Forest Service (Hunsaker and Eagan, 2003). The Southern Sierra CZO lies outside the limits of recent glaciation and is characterized by a sequence of parallel ridges and valleys, with alternating steep and gentle terrain of granitic bedrock. We focused on site P301 at the head of Providence Creek, which has a montane-steppe climate with a MAT of 9°C and a MAP of 1,100 mm year⁻¹ (Table 1). The topography is a 0.75 km wide valley with moderate to steep relief. Vegetation is dominated by a mixed-coniferous forest consisting of *Abies concolor*, *Pinus ponderosa*, *Pinus jeffreyi*, *Quercus kelloggii*, *Pinus lambertiana*, and *Calocedrus decurrens*, with intermixed chaparral. Eleven samples were collected using a Geoprobe® every 1.0 m down to 11.0 m in 2011 (Holbrook et al., 2014). Based upon the shallow depth of soil and high variability in regolith depth consistent with chemical weathering-limited regolith formation, we consider regolith at Southern Sierra CZO to be weak to moderately weathered (Bales et al., 2011). Stream water samples were collected above baseflow conditions from Providence Creek 301 in March and April of 2017 (see Godsey and Kirchner, 2014) using acid washed HDPE bottles following USGS water sampling techniques (United States Geological Survey [USGS], 2006).

Elemental Analyses

Extractions and Total Digestions of Regolith Samples

A two-step sequential extraction was performed to quantify organic bound and secondary oxide fractions. Subsamples of regolith from the four CZOs were dried at 105°C and then

pulverized in a boron carbide mortar and pestle to <100 μm. Two grams of regolith was weighed into 50 mL centrifuge tubes. First, organic matter and amorphous oxide bound elements were collected by adding 5 mL of 30% H₂O₂ to oxidize organic matter and then extracting the soil solution with 10 mL of 0.01 M acetic acid to target amorphous and short-range-ordered Al-, Mn-, and Fe- (oxyhydr)oxides. The solution was centrifuged at 7,000 rpm for 45 min and decanted. This was repeated with two washes of 10 mL of deionized water, which were added to the total extract. For the secondary Fe oxide fraction of Mo, Cr, and V, the remaining soil was treated with citrate-bicarbonate-dithionite (CBD) following the methods described in Mehra and Jackson (1960), which focuses on the dissolution of crystalline Fe oxides such as goethite and hematite without dissolution of Fe-bearing silicates. In brief, 40 mL of analytical grade 0.3 M sodium citrate and 5 mL of analytical grade 1 M sodium bicarbonate was added to the dry samples. The tubes were heated to 60°C and 1 g of analytical grade sodium dithionite was added. After 45 min of reaction, samples were centrifuged at 3,500 rpm for 30 min and the supernatant was collected, filtered to <0.4 μm, and diluted with deionized water. For every batch of samples, a blank, duplicate, and a standard reference material (SRM) was included. Montana Soil 2711 from the National Institute of Standards and Technology was used as a standard reference material (SRM).

For total sample digestion, 100 mg of dried, pulverized regolith were dissolved in 5 mL of 25 M HF acid and 5 mL of distilled 16 M HNO₃ (Trace metal grade, VWR Analytical, Radnor, PA, United States) at 130°C in sealed 30 mL Teflon PFA vials for 48 h or longer as needed with quartz-rich samples. After complete digestion of visible materials, samples were dried to a powder and redissolved in 0.5 M HNO₃. For every batch of samples, a blank, duplicate, and two SRMs [W-2 diabase and G-2 granite from the United States Geological Survey (USGS)] were included with every 20 samples to monitor reproducibility.

ICP-MS Analyses

Regolith digests and extracts were diluted with deionized water and analyzed for trace metals with an Element 2 ICP-MS (Thermo-Scientific, Waltham, MA, United States). Recoveries for total digests of Mo, V, Cr, Fe, and Ti were 81–103% of certified values. The variation between intra-sample duplicates was <6% and Ti

concentrations in the preparation blank samples were $<0.01 \mu\text{g g}^{-1}$.

Stream water samples were collected from each CZO under baseflow conditions between February and April 2017. Stream water samples were collected using acid-washed LDPE plastic bottles, filtered to $<0.45 \mu\text{m}$ and acidified to pH 1 with trace metal grade HNO_3 . Stream water samples were analyzed for trace metals using an Agilent 8800 triple quadrupole (QQQ) ICP-MS at the Dartmouth College Trace Element Analysis Laboratory (Agilent Technologies, Santa Clara, CA, United States). The QQQ-ICP-MS was calibrated using NIST traceable single and multi-element standards containing Sc, Ge, Y, In, Rh, Te, and Bi as internal standards. Ten point calibration curves were constructed for each analyte with correlation coefficient criteria >0.99 . The calibration was followed by an Initial Calibration Blank (IBC) and an Initial Calibration Verification (ICV). Acceptance criteria for the ICV and CCV are $\pm 10\%$. The CCV was run after every 10 samples. Analytical duplicates and spikes were performed every 20 samples. Spike recoveries were 93–101% for Mo, 91–99% for Cr, and 95–102% for V. Coefficient of variations (CVs) for duplicates were $<5\%$ for Mo, Cr, V, Fe, and Ti.

Micro X-Ray Fluorescence Mapping

The goal of the synchrotron-based Micro X-ray Fluorescence analysis (μ -XRF) was to elucidate whether V and Cr were located in primary minerals or secondary Fe oxide minerals. Molybdenum was not imaged due to its low concentration. Intact regolith samples were only collected from the Guaba Ridge site of the Luquillo CZO in February 2017 at the soil-regolith interface (1.8 m depth). The regolith sample was oven dried at 70°C and cemented in place using a room-temperature-curing epoxy-resin (EPO-TEK 301-2FL). The hardened soil columns were cut into 15 mm thick sections and wet polished using silicon carbide starting at 240 grit. Minimizing the amount of deionized water and decreasing the total amount of time samples spent wet-polished were taken to limit dissolution or disturbance of minerals, particularly the weathered rind, and water soluble elements. The weathering zone of the regolith was analyzed by μ -XRF imaging at the Cornell High Energy Synchrotron Source (CHESS) on the F3 bending-magnet beamline. At CHESS, a $20 \mu\text{m}$ beam (incident energy of 17 KeV) with an incident flux of $\sim 3 \times 10^9$ photons s^{-1} at the sample was used. The detector was mounted at 90° with respect to the incident X-ray beam and samples were mounted at 45° to the incident beam and scanned through the X-ray beam. The Vortex silicon drift detector with a Digital X-ray Processor (DXP) for digital signal processing to detect fluorescent X-rays. X-ray spectra were fitted for elements and quantified using the PyMCA software package (Solé et al., 2007).

Total Carbon Quantification

Soil carbon data was obtained for each CZO: Calhoun (Fimmen et al., 2008; Bacon et al., 2012), Luquillo (Buss et al., 2005), and Southern Sierra (Tian, 2018). Total organic C (TOC) concentrations in soil and regolith samples were measured for

Boulder Creek CZO samples using a Carlo-Erba Elemental Analyzer. In brief, $6 \pm 1 \text{ mg}$ subsamples $<0.5 \text{ mm}$ were combusted. Every 20 samples included one blank, one Atropine SRM, and a duplicate. TOC concentrations in Atropine SRMs were within 3% of its certified value and $<10\%$ relative percent difference. Soils were treated with 0.1 mM HCl acid to remove C from carbonates. Values for Boulder Creek CZO were comparable with surface soils from Eilers et al. (2012).

Data Analyses

We tested the associations of TOC and secondary Fe oxide with total Mo, V, and Cr concentrations and concentrations within secondary Fe oxide phase using linear regressions for each CZO. All regressions were performed using Matlab (Matlab, 2016, Mathworks, Natick, MA, United States). For elemental concentrations, error bars were propagated based upon the coefficient of variation for each sample measurement and the standard error measured through duplicate and triplicate samples.

Mass transfer coefficients (τ) of Mo, V, and Cr were calculated to assess the degree of chemical weathering for specific elements using Ti as an index element (Brantley and Lebedeva, 2011). Mass transfer coefficients are defined for the element of interest (Mo, V, and Cr) (j) in the soil or regolith sample normalized to an immobile index element Ti (i) in the parent material:

$$\tau_{j,w} = \frac{C_{j,w}C_{i,p}}{C_{j,p}C_{i,w}} - 1 \quad (1)$$

where $C_{j,w}$ and $C_{i,w}$ are total concentrations of the element of interest (Mo, V, and Cr) and Ti in the soil and regolith samples, respectively, and $C_{j,p}$ and $C_{i,p}$ are the element of interest and index element concentrations in the least weathered regolith material (e.g., Brimhall and Dietrich, 1987; Kraepiel et al., 2015). Negative τ values indicate a net loss of an element from a specific soil depth due to leaching. Positive τ values indicate a net enrichment of an element. Although Ti can be mobilized at strongly acidic, heavily weathered tropical soils (Kurtz et al., 2000), application of Ti-based mass transfer coefficients is effective for estimating relative losses and gains in the CZOs of our study.

Stream water concentrations were grouped across collection dates and compared across the four CZOs using the Kruskal-Wallis non-parametric tests. Using measured watershed area and mean annual stream discharge, we calculated the export of Mo, V, and Cr at each of the four CZOs. To accomplish this, we obtained the total watershed area, MAP, and mean annual discharge for each of the four CZOs from existing online data¹ (accessed May 2018). Stream water Mo, V, and Cr concentrations were multiplied by total discharge to estimate export rates for each element.

¹criticalzone.org

RESULTS

Regolith Profiles

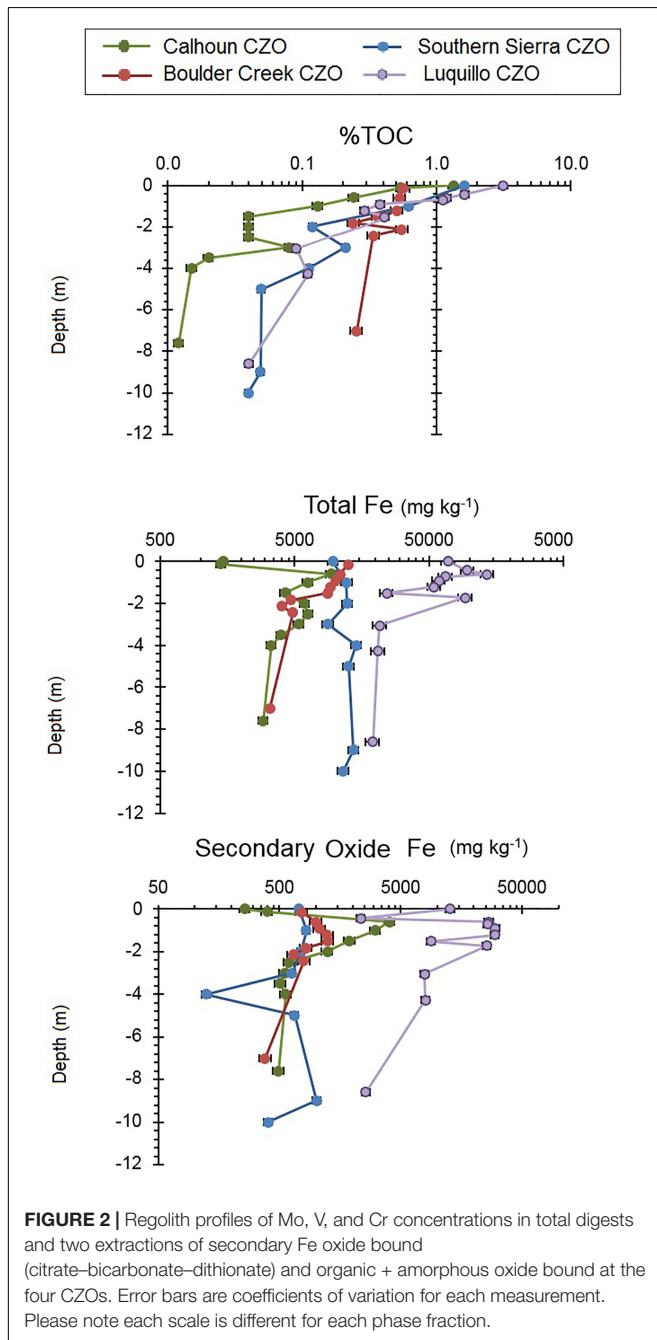
Regolith profiles exhibited a range of TOC and secondary oxide Fe with depth across the four CZOs. Overall, %TOC decreased with depth from approximately 1% down to 0.1% with subsurface peaks present at all four CZOs (Figure 2). Calhoun CZO had <0.1 %TOC below 2 m depth, which was lower than the other three CZOs (Figure 2). Total Fe was relatively constant with depth at Boulder Creek and Southern Sierra CZOs. Subtropical Calhoun CZO had low total Fe concentrations in the surface soils

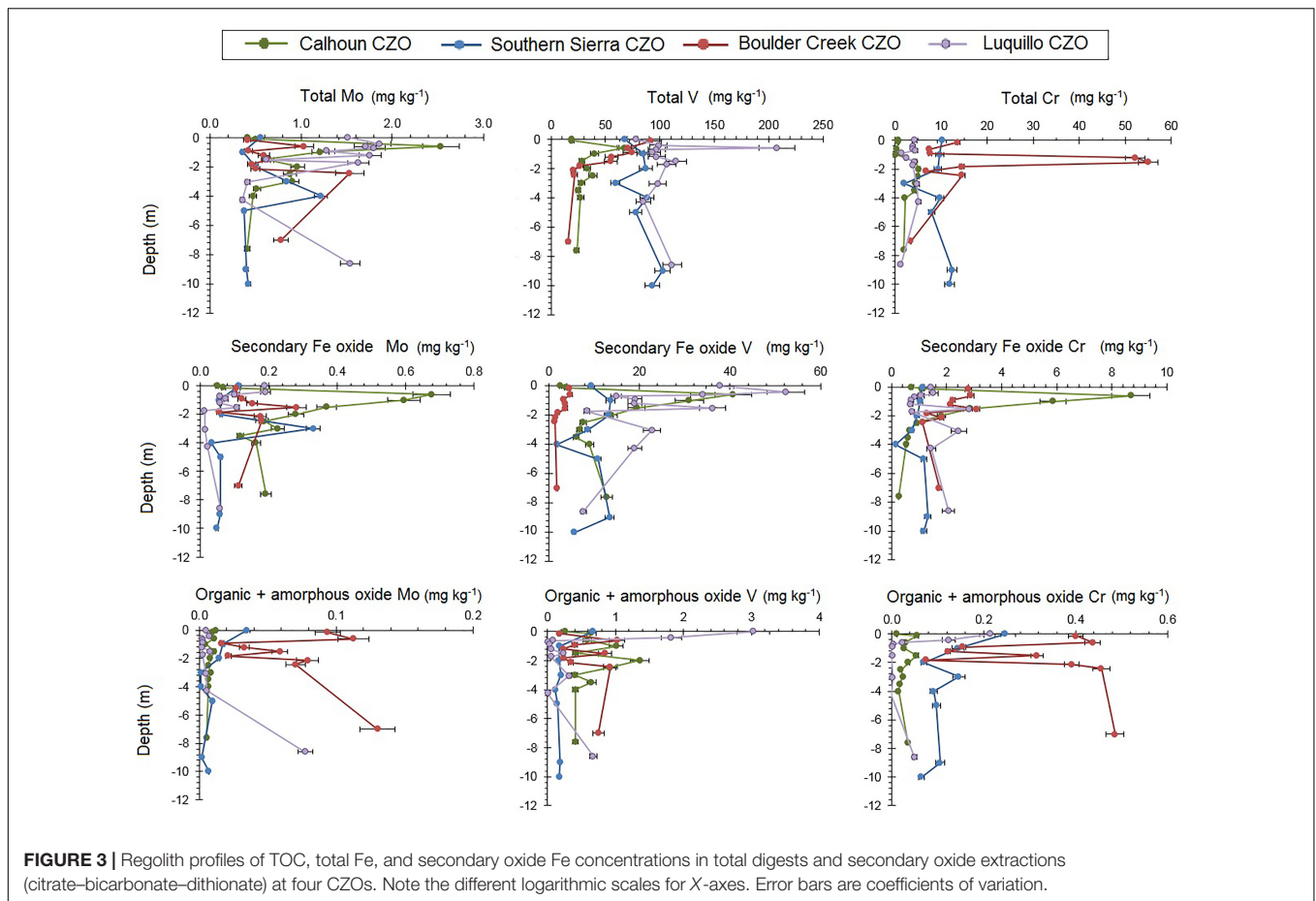
while tropical Luquillo CZO had higher total Fe concentrations above 2 m depth (Figure 2). Secondary oxide Fe concentrations were highest throughout the regolith profile at Luquillo CZO by nearly two orders of magnitude compared to Boulder Creek and Southern Sierra CZOs (Figure 2). Calhoun CZO had a subsurface peak of secondary oxide Fe concentration between 1 and 1.5 m depth (Figure 2).

Total Mo profile concentrations ranged from 0.4 to 2.5 mg kg⁻¹ across the four CZOs (Figure 3 and Supplementary Table 1). The highest total Mo concentrations at the Calhoun and Luquillo CZOs were in the surface soils, at 0.6 m and 0.4 m in depth, respectively. The colder, higher elevation Boulder Creek and Southern Sierra CZOs had their highest total Mo concentrations deeper in the regolith, at 2.4 m and 4 m in depth, respectively. Total V profiles exhibited two orders of magnitude variation in concentrations across regolith profiles. Total V concentrations were highest in the top meter for Boulder Creek, Luquillo, and Calhoun CZOs, and were generally consistent with depth at the Southern Sierra CZO. Total Cr concentrations at the Calhoun CZO had subsurface peaks of total Cr between 2.0 and 4.0 m. Boulder Creek exhibited a significant total Cr peak between 1.0 and 2.0 m, which decreased with depth. Southern Sierra and Luquillo CZO exhibited nearly homogeneous (± 3 mg kg⁻¹) total Cr profiles with depth.

In the regolith, organic matter and amorphous oxide bound Mo, V, and Cr were substantially lower than their respective secondary oxide and total concentrations. Across the four CZOs, organic matter and amorphous oxide bound Mo ranged between 0.01 and 0.13 mg kg⁻¹ (Supplementary Table 2), which on average was 0.5–0.9% of the total Mo concentration (Supplementary Table 4). The organic matter and amorphous oxide bound fraction of Mo were greatest near the surface (<1 m depth) for Calhoun and Southern Sierra CZOs while Boulder Creek and Luquillo CZOs had subsurface peaks (>2 m depth). Vanadium varied between 0.11 and 3.1 mg kg⁻¹ (Supplementary Table 2), which on average was 0.3–2.1% of the total V concentration (Supplementary Table 4). The organic matter and amorphous oxide bound fraction of V were greatest near the surface (<1 m depth) for Luquillo and Southern Sierra CZOs while Boulder Creek and Calhoun CZOs exhibited subsurface peaks (Figure 3). Organic bound Cr concentrations ranged between 0.01 and 1.07 mg kg⁻¹ (Supplementary Table 2), which on average was 0.9–3.5% of the total Cr concentration (Supplementary Table 4). Organic matter and amorphous oxide bound Cr was greatest in the top 2 m of regolith at Luquillo and Southern Sierra CZOs but were greater below 2 m in depth at Boulder Creek and Calhoun CZOs (Figure 3).

Secondary Fe oxide Mo concentrations ranged between 0.02 and 0.68 mg kg⁻¹ (Supplementary Table 3), which on average was 6.6–40.1% of the total Mo concentration (Supplementary Table 5). Vanadium concentrations in the secondary Fe oxide ranged between 1 and 52 mg kg⁻¹ (Supplementary Table 3), which on average was 6.0–39.7% of the total V concentration (Supplementary Table 5). Secondary Fe oxide Cr concentrations varied between 0.2 and 8.7 mg kg⁻¹, which on average was 13.0–40.5% of the total Cr concentrations (Supplementary Table 5).





Using Pearson correlations, we observed that total Mo, V, and Cr were correlated with secondary oxide Fe concentrations [a proxy for long-range ordered to crystalline Fe oxy(hydr)oxides] (Table 2). At Calhoun CZO, secondary oxide and total Mo, V, and Cr concentrations were positively correlated with secondary oxide Fe concentrations. For Southern Sierra CZO, secondary oxide V and Cr were positively correlated with secondary oxide Fe concentrations. At Boulder Creek CZO, secondary oxide and total concentrations of V and Cr were negatively correlated with both secondary oxide Fe and TOC. At Luquillo CZO,

secondary oxide Mo and V were positively correlated with %TOC.

Mass Transfer Coefficients and μ -XRF Mapping

Calculated tau values for Mo, V, and Cr show both net enrichment and depletion across the CZOs (Figure 4). At the montane coniferous Boulder Creek CZO, regolith down to 2.0 m depth were depleted in Mo and V, but Cr was enriched below 1.0 m

TABLE 2 | Pearson correlation coefficients for linear regressions between secondary Fe oxide and %TOC with secondary Fe oxide and total Mo, V, and Cr at each of the four CZOs.

Study area		Secondary oxide Mo	Secondary oxide V	Secondary oxide Cr	Mo total	V total	Cr total
Calhoun CZO	Secondary oxide Fe	1.0**	1.0**	1.0**	0.9**	0.9**	0.6*
	% TOC	-0.3	-0.2	-0.1	-0.1	-0.3	-0.3
Southern Sierra CZO	Secondary oxide Fe	0.1	0.9**	0.8*	-0.7*	0.5*	0.5*
	% TOC	0.1	0.1	0.2	-0.1	-0.4	0.1
Boulder Creek CZO	Secondary oxide Fe	0.4	0.6*	0.5*	-0.1	0.5*	0.7*
	% TOC	0.1	0.6*	0.6*	-0.2	0.6*	0.6*
Luquillo CZO	Secondary oxide Fe	-0.1	-0.2	-0.8*	0.4	0.3	-0.2
	% TOC	0.8*	0.6*	-0.2	0.4	0.0	0.3

** indicates $P < 0.01$ and * indicates $P < 0.05$.

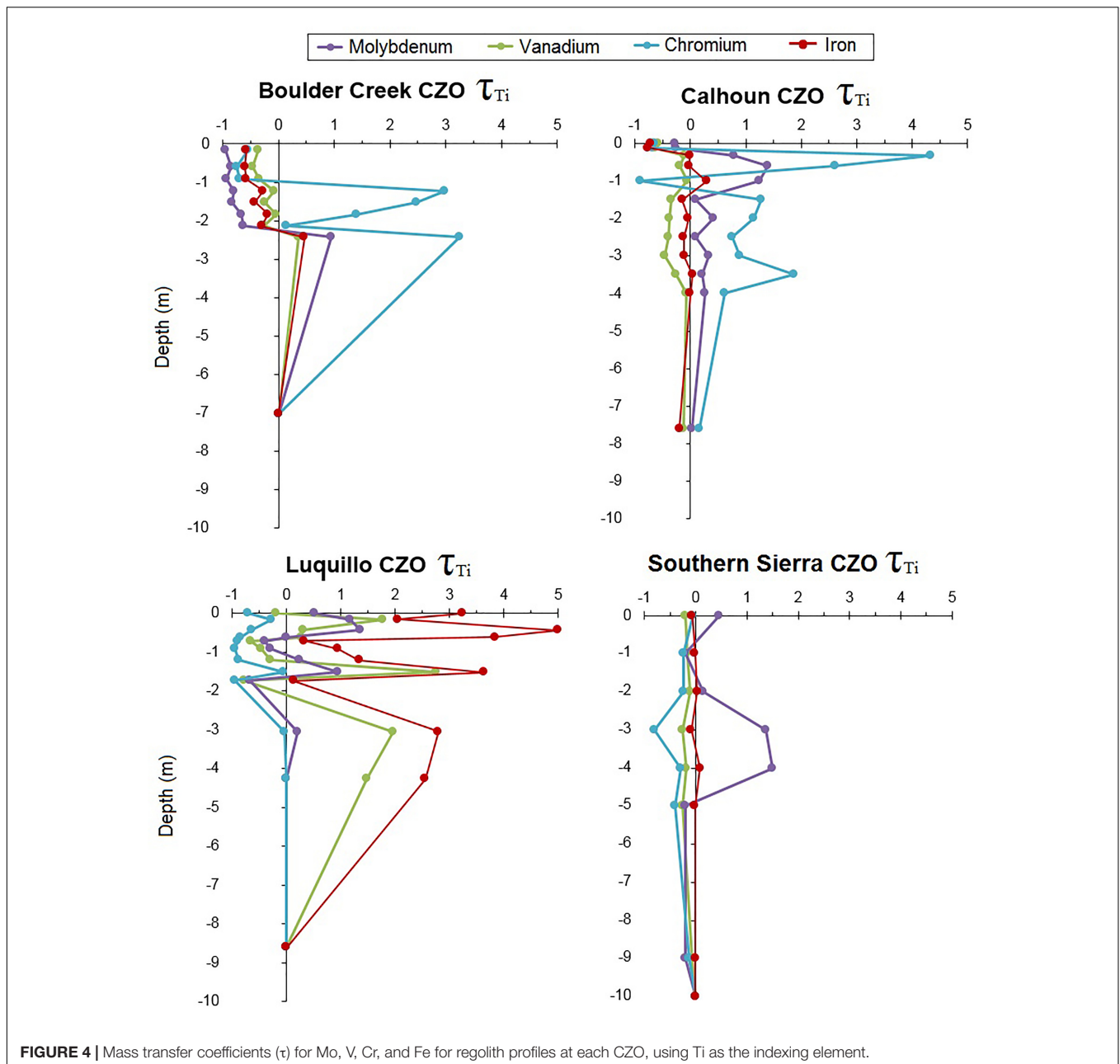


FIGURE 4 | Mass transfer coefficients (τ) for Mo, V, Cr, and Fe for regolith profiles at each CZO, using Ti as the indexing element.

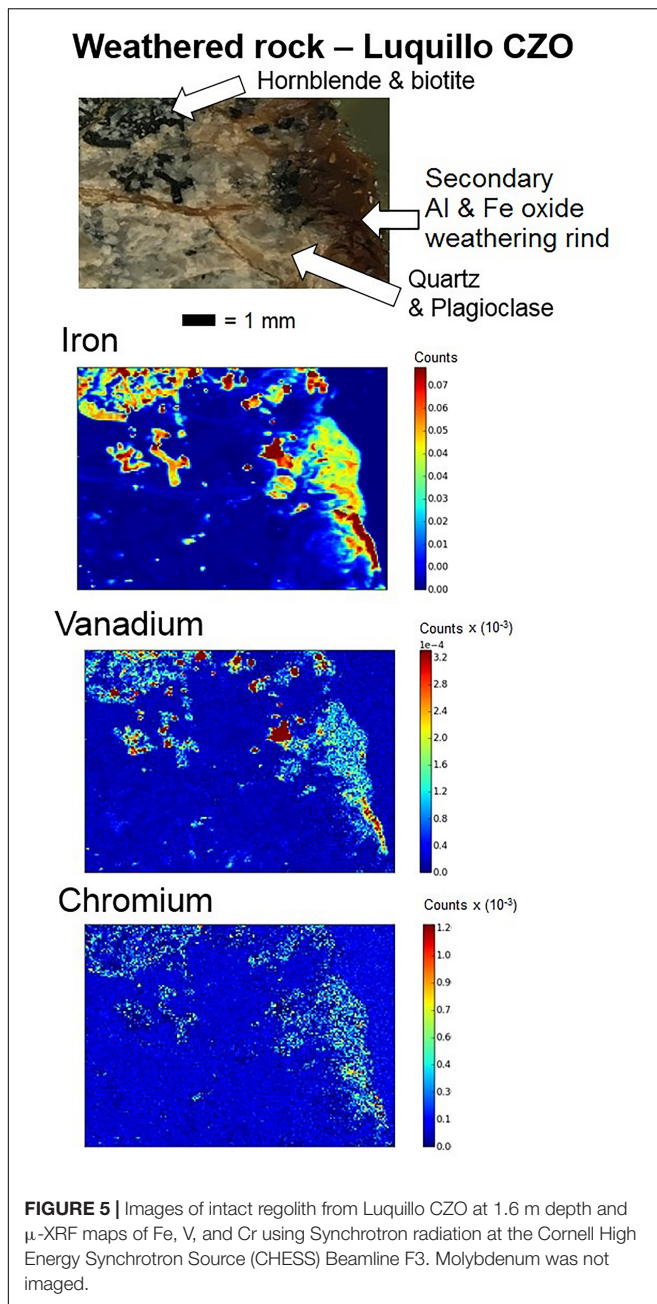
depth. At the subtropical Calhoun CZO, V was depleted while Mo and Cr were enriched throughout the regolith profile. The tropical Luquillo CZO showed a wide variation but overall Cr was depleted throughout the entire profile while Mo and V were enriched at certain depths. The Southern Sierra CZO regolith profile was depleted in V and Cr but enriched in the surface and subsurface between 2.0 and 5.0 m depth.

Analysis of the μ -XRF spectra for the weathered regolith from Luquillo CZO showed Fe, V, and Cr coinciding together in hornblende and biotite primary minerals (Buss et al., 2005, 2017). This is particularly observable in the upper left-hand corner of the images and the outlines of the hornblende minerals are distinguishable in all four images. Moreover, Fe, V, and Cr also

correspond with each other in the Fe oxide weathering rind on the right side of the image (Figure 5). More information on the weathering rinds of quartz diorite from Luquillo CZO is available in Buss et al. (2008).

Stream Water Concentrations

Overall, stream water concentrations of oxyanions were generally comparable across CZOs (Table 3 and Figure 6), but there were a few significant differences. Stream water V concentrations were similar across CZOs and ranged between 0.04 and 0.70 $\mu\text{g L}^{-1}$ (Figure 6). Stream water Cr concentrations at Calhoun and Boulder Creek CZOs were significantly than at the Southern



Sierra and Luquillo CZOs (Table 3 and Figure 6) using the non-parametric Kruskal–Wallis Test ($p < 0.05$). Stream water Mo concentrations were significantly higher at Boulder Creek and Calhoun CZOs compared to Southern Sierra CZO ($p < 0.05$, Table 3 and Figure 6).

We compared the concentration of oxyanions in the stream water to the deepest, least weathered regolith to determine if variations in lithology explained the differences in stream water concentrations across CZOs and among oxyanions. In Figure 7, Mo stream water to regolith ratios were significantly greater at subtropical Calhoun and tropical Luquillo CZOs than montane Southern Sierra and Boulder Creek CZOs. In addition, Mo stream

water to regolith ratios at Calhoun, Luquillo, and Southern Sierra CZOs were significantly greater than V and Cr ratios. Stream water to regolith ratios for V were not significantly different for Boulder Creek, Calhoun, and Luquillo CZOs but were greater than at Southern Sierra CZO. In addition, Stream water to regolith ratios for V were generally lower than Mo and Cr across CZOs (Figure 7). Stream water to regolith ratios for Cr were significantly higher at Calhoun CZO than the other three CZOs. Similarly, stream water to regolith ratios for Cr were significantly higher at Boulder Creek CZO than Luquillo and Southern Sierra CZOs.

DISCUSSION

Weathering and Partitioning of Mo, V, and Cr

Our results support the hypothesis that deep regolith play a substantial role in sorption of oxyanions. Overall, both surface soils (<0.3 m depth) and deeper regolith served as important sources and retainers of oxyanions. We observed many peaks in Mo, V, and Cr in both the organic matter and amorphous oxide and the secondary Fe oxide extractions at depths are far deeper than typical 0.3–1 m depth investigated for oxyanion sorption and weathering in soils (e.g., Shiller and Mao, 2000; Wichard et al., 2009; Wisawapipat and Kretzschmar, 2017). For example, at the montane regolith of Southern Sierra CZO had >39% of Mo and Cr were in the secondary Fe oxide fraction from 3 to 4 m in depth and the tropical forest Luquillo CZO, 52% of Cr and 23% of V were in the secondary Fe oxide fraction at 3 m in depth.

In addition, enrichment and depletion of oxyanions >2 m in depth indicated that regolith played both a significant role in the sorption and retention of oxyanions (Figure 4). Except for Cr, Boulder Creek CZO demonstrated the most depletion of oxyanions, extending down 2 m in depth (Figure 4). This is particularly important as the mountain-steppe Boulder Creek CZO has the least intensive weathering environment with the lowest MAP and MAT, but due to its long exposure, has been moderate to extensively weathered. The more tropical regolith profiles at Calhoun and Luquillo CZOs show much more complicated patterns of accumulation and depletion (Figure 4), likely due to variations in retention as described later in this section.

These results support other weathering observations by Dethier and Bove (2011) at Boulder Creek CZO, Bacon et al. (2012) at Calhoun CZO, and Buss et al. (2005) at Luquillo CZO. Subtropical Calhoun CZO and tropical Luquillo CZO were the most weathered regolith profiles and had the highest accumulations of secondary Fe oxides (Figure 2), consisting of hematite and goethite as observed by Buss et al. (2005); Fimmen et al. (2008), and Dethier and Bove (2011). In addition, neoformed kaolinite was present at the previously mentioned CZOs at >4% by mass (Fimmen et al., 2008 at Calhoun CZO; Dethier and Bove, 2011 at Boulder Creek CZO; Buss et al., 2017 at Luquillo CZO) demonstrating their extensive weathering history. The extent of weathering corresponded with the sorption of oxyanions throughout the regolith profiles. Southern Sierra had

TABLE 3 | Stream water export estimates for dissolved Mo, V, and Cr across the four CZOs.

	Boulder Creek CZO Gordon Gulch watershed	Calhoun CZO Watershed 4	Luquillo CZO Rio Icaeos watershed	Southern Sierra CZO Providence Creek
Watershed size (km ²)	2.77	0.07	3.14	0.99
Mean annual precipitation (m)	0.74	1.25	4.20	1.10
Water annual flux (m ³)	$2.4 \times 10^5 \pm 1.2 \times 10^5$	$2.5 \times 10^4 \pm 1.7 \times 10^4$	$1.3 \times 10^7 \pm 3.1 \times 10^6$	$4.0 \times 10^5 \pm 3.4 \times 10^4$
Mean Mo concentrations ($\mu\text{g L}^{-1}$)	0.06 ± 0.01	0.08 ± 0.02	0.06 ± 0.03	0.02 ± 0.01
Mean V concentrations ($\mu\text{g L}^{-1}$)	0.50 ± 0.04	0.43 ± 0.0	0.60 ± 0.24	0.33 ± 0.05
Mean Cr concentrations ($\mu\text{g L}^{-1}$)	0.27 ± 0.02	0.18 ± 0.03	0.08 ± 0.02	0.10 ± 0.01
Mo flux [†] (mg year ⁻¹)	$9.8 \times 10^2 \pm 4.3 \times 10^2$	$1.9 \times 10^3 \pm 5.1 \times 10^2$	$1.2 \times 10^6 \pm 4.1 \times 10^5$	8.0 ± 2.5
V flux [†] (mg year ⁻¹)	$8.4 \times 10^3 \pm 2.9 \times 10^3$	$1.1 \times 10^4 \pm 3.1 \times 10^3$	$7.8 \times 10^6 \pm 2.2 \times 10^6$	$1.3 \times 10^2 \pm 4.9 \times 10^1$
Cr flux [†] (mg year ⁻¹)	$9.3 \times 10^3 \pm 3.7 \times 10^3$	$4.4 \times 10^3 \pm 1.2 \times 10^3$	$6.5 \times 10^5 \pm 3.4 \times 10^5$	40 ± 18

Averages are given \pm one standard error. [†]The flux estimates are based upon baseflow oxyanion concentrations. Here, we assumed oxyanions were isostatic, which may not necessarily be applicable for each element at all of the CZOs.

lower secondary Fe oxide fractions of Mo, Cr, and V compared to the other three CZOs. Moreover, secondary oxide Mo, Cr, and V were greater in regolith with higher secondary Fe oxide concentrations at much warmer and wetter Calhoun and Luquillo CZOs when compared to the colder and drier Boulder Creek CZO. Thus, we conclude that weathering has influenced the formation and retention of oxyanions with secondary Fe oxides.

A generalized trends across the three oxyanions were present, demonstrating some linkages between weathering intensity and climate with the sorption of oxyanions to secondary Fe oxides. Total Mo, secondary Fe-bound Mo and organic and amorphous oxide bound Mo concentrations were comparable across the four CZOs, suggesting weathering intensity nor lithology did not strongly influence Mo in the soil and regolith profiles. Secondary oxides did not appear to play a dominant role for Mo retention at Luquillo CZO as total Mo was not correlated with secondary Fe oxides. Instead secondary oxide Mo was correlated with %TOC despite the fact that organic matter and amorphous oxide bound Mo was not a substantial fraction of the total Mo concentrations at any of the CZOs, generally ranging below 5%. This largely agrees with previous studies that the sorption and retention of Mo is dominated by both, secondary Fe oxides and organic compounds (e.g., Wichard et al., 2009; King et al., 2016, 2018). Due to the relatively small range in %TOC, there may not have been enough variability to capture the relationship between Mo and TOC.

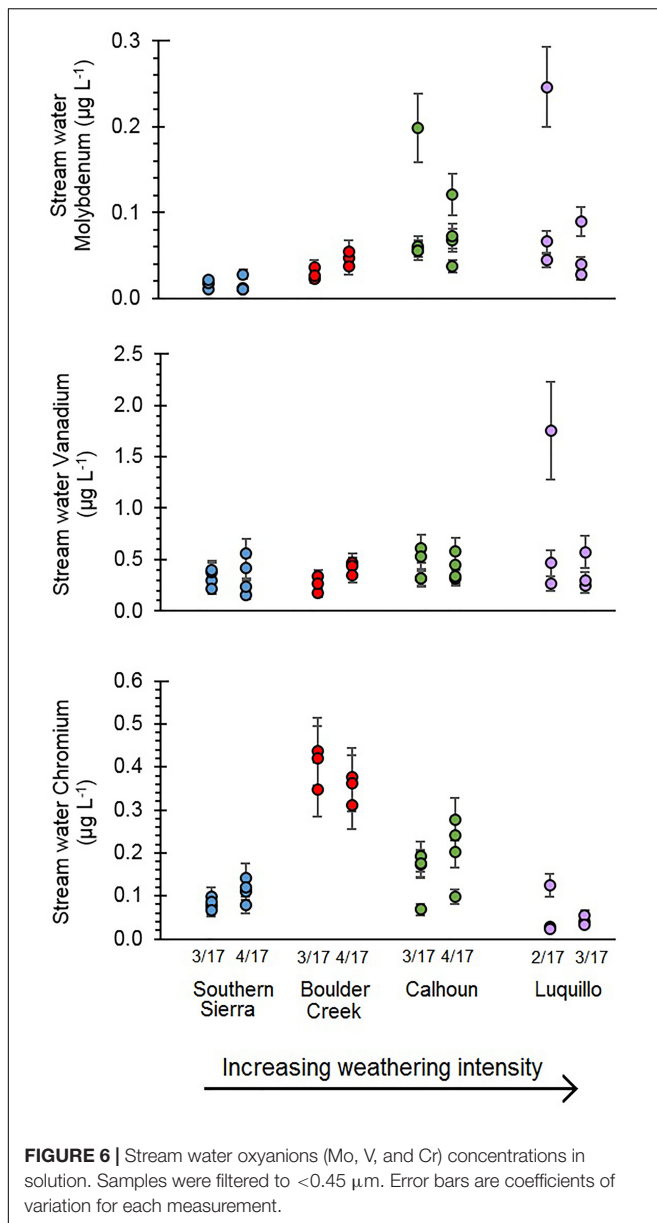
Total V concentrations varied significantly across the CZOs (**Supplementary Table 1**), suggesting lithologic controls on the sourcing of V to the soil and regolith profiles. Secondary Fe oxide fraction of V, however, coincided with weathering intensity. Average secondary Fe oxide concentrations were highest for the more tropical Calhoun (14 mg kg^{-1}) and Luquillo CZO (26 mg kg^{-1}) compared to mountain-steppe Southern Sierra (9 mg kg^{-1}) and Boulder Creek CZOs (3 mg kg^{-1}). Vanadium exhibited significant linear relationships with secondary Fe oxide at Calhoun, Boulder Creek, and Southern Sierra CZOs. The substitution of V(III) for Fe(III) in minerals has been widely observed (Schwertmann and Pfab, 1996; Shiller and Mao, 2000; Wisawapipat and Kretzschmar, 2017) and V(II) and V(III) for Fe(II) and Fe(III) in primary Fe-silicate minerals during

magmatic crystallization (e.g., Goldschmidt, 1954). Even though this relationship was not clearly observed at Luquillo CZO as with the other three CZOs using linear regressions with secondary Fe oxide, we did observe this relationship in μ -XRF maps of regolith samples. Our μ -XRF imaging of V in an intact weathering rind sample from Luquillo demonstrates its spatial distribution with Fe, both in primary minerals like hornblende and biotite and in secondary Fe oxides within regolith at Luquillo CZO.

Chromium concentrations exhibited a pattern similar to V. Total Cr concentrations were varied strongly with lithology but Cr concentrations in secondary Fe oxides appeared to be climate influenced. The more tropical Calhoun and Luquillo CZOs had higher % Cr in the secondary Fe oxide fraction than the montane-steppe Southern Sierra and Boulder Creek CZOs, suggesting intensive weathering promotes Cr sorption by secondary Fe oxides. The sorption of Cr by secondary Fe oxides and organic matter has been well observed by previous studies (e.g., Gustafsson et al., 2014; Pérez et al., 2014; Saputro et al., 2014).

Some potential variables that may explain the variation of oxyanions not explored here are the effects of erosion, atmospheric inputs, hydrological properties, and other source of sorption such as clay minerals and other oxides. Luquillo CZO differs from the other three CZOs due to its substantially greater annual precipitation (**Table 1**), which could not only flush and dissolve solutes at rates that may prevent sorption (see Dosseto et al., 2012) but also lead to increased atmospheric inputs of oxyanions in the surface soils (Marks et al., 2015; King et al., 2016). This may also influence τ values by enriching oxyanions at the surface and a net depletion due to leaching losses with depth. Nevertheless, the effect of atmospheric inputs on the deep regolith is likely minimal. In addition, Luquillo CZO undergoes more erosion in the form of landslides and surface soil erosion than the other three CZOs (Larsen, 2012). Lastly, Luquillo CZO also had much greater clay content in its soils and upper regolith than Calhoun, Boulder Creek, and Southern Sierra CZOs. Clays can provide an unaccounted source of oxyanion sorption capacity (Goldberg et al., 1996).

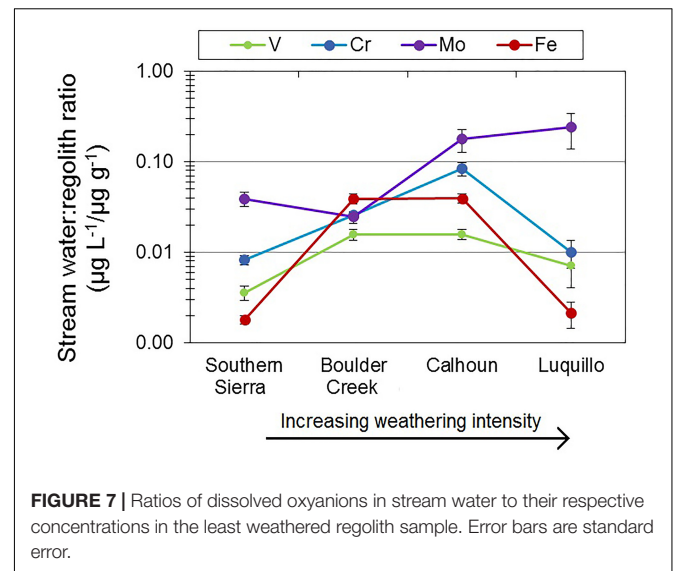
Our study observed low fractions of oxyanions in the organic bound and amorphous oxide phase and poor correlations



between %TOC and oxyanion concentrations in the deep regolith. However, this conclusion should not be extrapolated to surface soils. Many previous studies have observed a significant relationship in surface soils and oxyanion concentrations (see Grove and Ellis, 1980; Wichard et al., 2009; King et al., 2014, 2016, 2018; Pérez et al., 2014; Marks et al., 2015; Siebert et al., 2015; King, 2017; Larsson et al., 2017; Wisawapipat and Kretzschmar, 2017). Therefore, sorption of oxyanions with organic matter may be most important spatially but not with depth into deep regolith ($>2 \text{ m}$).

Stream Water Export of Mo, V, and Cr

Oxyanion concentrations and export from the Critical Zone via stream water varied substantially across CZOs. The most intensively weathered regolith had higher average Mo



concentrations in stream water (Table 3 and Figure 6). However, Mo concentrations were generally comparable across CZOs when removing the outlier samples at Calhoun and Luquillo CZOs. Calhoun and Luquillo CZOs had higher Mo stream water to regolith ratios compared to V and Cr (Figure 7). This implies that Mo had lower relative retention in regolith, increasing its export by stream water compared to V and Cr at Calhoun and Luquillo CZOs. Alternatively, the stream water to regolith ratios increase with increasing MAP across the CZO (Table 1 and Figure 7). This suggests that atmospheric inputs of Mo via precipitation (Marks et al., 2015; Siebert et al., 2015; King et al., 2016) may lead to increased export of Mo from the regolith. There may be additional transport processes influencing Mo transport such as colloidal Al, Fe, and Mn oxides and dissolved organic matter (Pearce et al., 2010; Trostle et al., 2016; Prouty et al., 2017), which can enhance its transport through soil. Furthermore, fine colloids $<0.45 \mu\text{m}$ in solution may also be responsible for the two elevated Mo concentrations at Calhoun and Luquillo CZOs. When these high concentrations are not considered, Mo concentrations were similar. Thus, there is not a strong trend in Mo concentrations with weathering intensity but potential variability due to colloids was greatest at the most intensively weathered CZOs.

Few studies have examined the controls on V concentrations in stream water (Shiller and Boyle, 1987; Shiller, 1997; Shiller and Mao, 2000; Strady et al., 2009). Stream water V concentrations were not significantly different across the four CZOs (Table 3). The similarity in stream water to regolith ratio for V suggests that regolith at Boulder Creek, Calhoun, and Luquillo CZOs are weathering and exporting V at consistent rates. Further, the stream water to regolith V ratios were lower than Mo and Cr, suggesting that V is the least mobile of the three oxyanions during weathering (Figure 7). The elevated stream water V concentration measured in one sample at Luquillo CZO may be due to colloids, particularly DOC and Al and Fe particulates. Stream water to regolith ratios for V was not significantly different than Fe for each CZO, suggesting V export is directly

controlled with Fe movement. This may be as either dissolved or fine colloids $<0.45 \mu\text{m}$, the size of the filter pores used in this study (e.g., Pokrovsky and Schott, 2002; Gardner et al., 2017). Stream water Cr concentrations exhibited the greatest variation among the four CZOs. Boulder Creek CZO had the highest stream water Cr concentrations (Table 3). Moreover, Boulder Creek CZO had significantly higher stream water to regolith ratio, despite having the lowest MAT and lowest MAP compared with the other four CZOs in this study (Figure 7).

Using measured watershed area and mean annual stream discharge, we calculated the export of Mo, V, and Cr at each of the four CZOs. Luquillo CZO had Mo, V, and Cr fluxes (10^5 to $10^6 \text{ mg year}^{-1}$) up to four orders of magnitude greater than the other CZOs (10^2 to 10^4 mg per year) due to 10^2 to 10^3 times greater stream discharge than the other three CZOs. We observed that Boulder Creek CZO had greater Mo, V, and Cr fluxes than Southern Sierra CZOs, despite having lower MAP. Even when scaled for different watersheds size, Boulder Creek had $>10\times$ greater export of oxyanions per km^2 . This highlights the importance that more weathered systems (based upon interpretation of mass transfer coefficients) export more oxyanions at greater rates than fresher regolith. It must be noted these approximations are based upon oxyanion concentrations in baseflow conditions. While this assumption might not hold for each of the oxyanions at the four CZOs, previous studies such as Shiller and Mao (2000), Aguirre et al. (2017) have found oxyanions can be isostatic with respect to concentration-discharge (CQ) dynamics. However, this provides an estimate in the variation of Mo, V, and Cr export via stream waters across different watershed with contrasting climates.

CONCLUSION

Our study has shown that retention and sourcing of Mo, V, and Cr from regolith extends far below the depth that most typical soil studies examine. Depletion of Mo, V, and Cr extends several meters in depth at all four CZOs, from the montane-steppe Boulder Creek CZO to the tropical rainforest Luquillo CZO. Moreover, secondary Fe oxides containing Mo, V, and Cr are present beyond surface soils, extending down $>8 \text{ m}$ in depth and were important fraction of the total percentage. In particular, $>25\%$ of total Cr and V were in the secondary Fe oxide fraction at Luquillo and Calhoun CZO between 0 and 2 m depth.

Each of the three oxyanions exhibited a unique pattern in stream water samples. Total concentrations and regolith to

stream water ratios of Mo and Cr exhibited significant variation among the four CZOs while V concentrations were similar across CZOs. Our regolith and stream water results highlight that each oxyanion has different geochemical pathways but share unifying principles across weathering and climate gradients. Identifying the upland causes for different oxyanion retention is key for developing Mo, V, and Cr as geochemical tools for understanding contemporary and paleo-terrestrial and marine global biogeochemical cycles.

AUTHOR CONTRIBUTIONS

JR conducted laboratory experiments, analyzed, and interpreted data and shaped discussion. EK analyzed and interpreted data and shaped discussion.

FUNDING

This work was made possible by the National Science Foundation Grant (NSF-1360760) to the Critical Zone Observatory Network National Office. Funding from the National Science Foundation for each CZO was also instrumental for each CZO studied in this project: Boulder Creek (NSF-1331828), Calhoun (NSF-1331846), Luquillo (NSF-1331841), and Southern Sierra (NSF-1331939).

ACKNOWLEDGMENTS

We are thankful for help with obtaining samples from Erin Stacy (UC Merced), Stephen Hart (UC Merced), Scott Hynek (Penn State), Sue Brantley (Penn State), and Andy Kurtz (Boston University). We are thankful for the UC Angelo Coast Range Reserve and the analytical help from Brian Jackson (Dartmouth College). CHESS is supported by the NSF and NIH/NIGMS via NSF award DMR-1332208, and the MacCHESS resource is supported by NIH/NIGMS award GM-103485.

SUPPLEMENTARY MATERIAL

The Supplementary Material for this article can be found online at: <https://www.frontiersin.org/articles/10.3389/feart.2018.00193/full#supplementary-material>

REFERENCES

- Adriano, D. C. (2001). *Trace Elements in Terrestrial Environments*. New York, NY: Springer, 219–261. doi: 10.1007/978-0-387-21510-5
- Aguirre, A. A., Derry, L. A., Mills, T. J., and Anderson, S. P. (2017). Colloidal transport in the Gordon Gulch catchment of the Boulder Creek CZO and its effect on C-Q relationships for silicon. *Water Resour. Res.* 53, 2368–2383. doi: 10.1002/2016WR019730
- Alloway, B. (2013). *Heavy Metals in Soil: Trace Metals and Metalloids in Soil and Their Bioavailability*. Reading: Springer. doi: 10.1007/978-94-007-4470-7
- Amundson, R., Richter, D. D., Humphreys, G. S., Jobbágy, E. G., and Gaillardet, J. (2007). Coupling between biota and earth materials in the critical zone. *Elements* 3, 327–332. doi: 10.2113/gselements.3.5.327
- Bacon, A. R., Richter, D. D., Bierman, P. R., and Rood, D. H. (2012). Coupling meteoric ^{10}Be with pedogenic losses of ^9Be to improve soil residence time estimates on an ancient North American interfluve. *Geology* 40, 847–850. doi: 10.1130/G33449.1
- Bales, R. C., Conklin, M. H., Kerkez, B., Glaser, S., Hopmans, J. W., Hunsaker, C. T., et al. (2011). “Sampling strategies in forest hydrology and biogeochemistry,” In *Forest Hydrology and Biogeochemistry: Synthesis of Past Research and Future*

- Directions*, eds D. F. Levia, D. Carlyle-Moses, and T. Tanaka (Dordrecht: Springer), 29–44. doi: 10.1007/978-94-007-1363-5_2
- Barnes, R. T., Smith, R. L., and Aiken, G. R. (2012). Linkages between denitrification and dissolved organic matter quality, boulder creek watershed, Colorado. *J. Geophys. Res.* 117:G01014. doi: 10.1029/2011JG001749
- Barron, A. R., Wurzbarger, N., Bellenger, J. P., Wright, S. J., Kraepiel, A. M. L., and Hedin, L. O. (2008). Molybdenum limitation of asymbiotic nitrogen fixation in tropical forest soils. *Nat. Geosci.* 2, 42–45. doi: 10.1038/nge0366
- Brantley, S. L., Goldhaber, M. B., and Ragnarsdottir, K. V. (2007). Crossing disciplines and scales to understand the critical zone. *Elements* 3, 307–314. doi: 10.2113/gselements.3.5.307
- Brantley, S. L., and Lebedeva, M. (2011). Learning to read the chemistry of regolith to understand the critical zone. *Annu. Rev. Earth Planet. Sci.* 39, 387–416. doi: 10.1146/annurev-earth-040809-152321
- Brimhall, G. H., and Dietrich, W. E. (1987). Constitutive mass balance relations between chemical composition, volume, density, porosity, and strain in metasomatic hydrochemical systems: results on weathering and pedogenesis. *Geochim. Cosmochim. Acta* 51, 567–587. doi: 10.1016/0016-7037(87)90070-6
- Buss, H. L., Bruns, M. A., Schultz, M. J., Moore, J., Mathur, C. F., and Brantley, S. L. (2005). The coupling of biological iron cycling and mineral weathering during saprolite formation, Luquillo Mountains, Puerto Rico. *Geobiology* 3, 247–260. doi: 10.1111/j.1472-4669.2006.00058.x
- Buss, H. L., Chapela Lara, M., Moore, O. W., Kurtz, A. C., Schulz, M. S., and White, A. F. (2017). Lithological influences on contemporary and long-term regolith weathering at the Luquillo critical zone observatory. *Geochim. Cosmochim. Acta* 196, 224–251. doi: 10.1016/j.gca.2016.09.038
- Buss, H. L., Sak, P. B., Webb, S. M., and Brantley, S. L. (2008). Weathering of the Rio Blanco quartz diorite, Luquillo Mountains, Puerto Rico: coupling oxidation, dissolution, and fracturing. *Geochim. Cosmochim. Acta* 72, 4488–4507. doi: 10.1016/j.gca.2008.06.020
- Buss, H. L., and White, A. F. (2012). “Weathering processes in the Icosos and Mameyes watersheds in eastern Puerto Rico,” in *Water Quality and Landscape Processes of Four Watersheds in Eastern Puerto Rico*, eds S. F. Murphy and R. F. Stallard (Reston, VA: U. S. Geological Survey), 249–262. doi: 10.3133/pp1789I
- Cantley, L. C., Cantley, L. G., and Josephson, L. (1978). A characterization of vanadate interactions with the (Na, K)-ATPase. Mechanistic and regulatory implications. *J. Biol. Chem.* 253, 7361–7368.
- Cantley, L. C., Josephson, L., Warner, R., Yanagisawa, M., Lechene, C., and Guidotti, G. (1977). Vanadate is a potent (Na, K)-ATPase inhibitor found in ATP derived from muscle. *J. Biol. Chem.* 252, 7421–7423.
- Chorover, J., Kretzschmar, R., Garcia-Pichel, F., and Sparks, D. L. (2007). Soil biogeochemical processes within the critical zone. *Elements* 3, 321–326. doi: 10.2113/gselements.3.5.321
- Condie, K. C., Dengate, J., and Cullers, R. L. (1995). Behavior of rare earth element in a paleoweathering profile. *Geochim. Cosmochim. Acta* 59, 279–294. doi: 10.1016/0016-7037(94)00280-Y
- Crans, D. C., Mahroof-Tahir, M., and Keramidis, A. D. (1995). “Vanadium chemistry and biochemistry of relevance for use of vanadium compounds as antidiabetic agents,” in *Vanadium Compounds: Biochemical and Therapeutic Applications*, eds A. K. Srivastava and J. L. Chiasson (Boston, MA: Springer), 17–24.
- Dayan, A. D., and Paine, A. J. (2001). Mechanisms of chromium toxicity, carcinogenicity and allergenicity: review of the literature from 1985 to 2000. *Human Exp. Toxicol.* 20, 439–451. doi: 10.1191/096032701682693062
- Dethier, D. P., and Bove, D. J. (2011). Mineralogic and geochemical changes from alteration of granitic rocks, boulder creek catchment, Colorado. *Vadose Zone J.* 10, 858–866. doi: 10.2136/vzj2010.0106
- Dosseto, A., Buss, H. L., and Suresh, P. O. (2012). Rapid regolith formation over volcanic bedrock and implications for landscape evolution. *Earth Planet. Sci. Lett.* 337, 47–55. doi: 10.1016/j.epsl.2012.05.008
- Eilers, K. G., Debenport, S., Anderson, S., and Fierer, N. (2012). Digging deeper to find unique microbial communities: the strong effect of depth on the structure of bacterial and archaeal communities in soil. *Soil Biol. Biochem.* 50, 58–65. doi: 10.1016/j.soilbio.2012.03.011
- Fimmen, R. L., Vasudevan, D., Williams, M. A., and West, L. T. (2008). Rhizogenic Fe–C redox cycling: a hypothetical biogeochemical mechanism that drives crustal weathering in upland soils. *Biogeochemistry* 87, 127–141. doi: 10.1007/s10533-007-9172-5
- Gäbler, H. E., Glüh, K., Bahr, A., and Utermann, J. (2009). Quantification of vanadium adsorption by German soils. *J. Geochem. Explor.* 103, 37–44. doi: 10.1016/j.gexplo.2009.05.002
- Garcia-Martino, A. R., Warner, G. S., Scatena, F. N., and Civco, D. L. (1996). Rainfall, runoff and elevation relationships in the Luquillo Mountains of Puerto Rico. *Caribb. J. Sci.* 32, 413–424.
- Gardner, C. B., Carey, A. E., Lyons, W. B., Goldsmith, S. T., McAdams, B. C., and Trierweiler, A. M. (2017). Molybdenum, vanadium, and uranium weathering in small mountainous rivers and rivers draining high-standing islands. *Geochim. Cosmochim. Acta* 219, 22–43. doi: 10.1016/j.gca.2017.09.012
- Geological Survey, U. S. (2006). *Collection of Water Samples (Ver. 2.0)*. Reston, VA: U.S. Geological Survey.
- Giardino, J. R., and Houser, C. (2015). *Principles and Dynamics of the Critical Zone*, Vol. 19. Waltham, MA: Elsevier.
- Godsey, S. E., and Kirchner, J. W. (2014). Dynamic, discontinuous stream networks: hydrologically driven variations in active drainage density, flowing channels and stream order. *Hydrol. Process.* 28, 5791–5803. doi: 10.1002/hyp.10310
- Goldberg, S., Forster, H. S., and Godfrey, C. L. (1996). Molybdenum adsorption on oxides, clay minerals, and soils. *Soil Sci. Soc. Am. J.* 60, 425. doi: 10.2136/sssaj1996.03615995006000020013x
- Goldschmidt, V. M. (1954). *Geochemistry*. Oxford: Oxford University Press, 730.
- Grove, J. H., and Ellis, B. G. (1980). Extractable chromium as related to soil pH and applied chromium. *Soil Sci. Soc. Am. J.* 44, 238–242. doi: 10.2136/sssaj1980.03615995004400020005x
- Gupta, U. C. (ed.). (1997). *Molybdenum in Agriculture*. Cambridge: Cambridge University Press, 276. doi: 10.1017/CBO9780511574689
- Gustafsson, J. P., Persson, I., Oromieh, A. G., van Schaik, J. W. J., Sjöstedt, C., and Kleja, D. B. (2014). Chromium(III) complexation to natural organic matter: mechanisms and modeling. *Environ. Sci. Technol.* 48, 1753–1761. doi: 10.1021/es404557e
- Holbrook, W. S., Riebe, C. S., Elwaseif, M., Hayes, J. L., Basler-Reeder, K., Harry, D. L., et al. (2014). Geophysical constraints on deep weathering and water storage potential in the Southern Sierra critical zone observatory. *Earth Surf. Process. Landf.* 39, 366–380. doi: 10.1002/esp.3502
- Hunsaker, C. T., and Eagan, S. M. (2003). “Small stream ecosystem variability in the Sierra Nevada of California,” in *First Interagency Conference on Research in the Watersheds*, eds K. G. Renard, S. A. McElroy, W. J. Gburek, H. E. Canfield, and R. L. Scott (Benson, AZ: U.S. Department of Agriculture), 716–721.
- Imtiaz, M., Rizwan, M. S., Xiong, S., Li, H., Ashraf, M., Shahzad, S. M., et al. (2015). Vanadium, recent advancements and research prospects: a review. *Environ. Int.* 80, 79–88. doi: 10.1016/j.envint.2015.03.018
- Kabata-Pendias, A. (2011). *Trace Elements in Soils and Plants*. Boca Raton, FL: Taylor and Francis Group.
- Kaiser, B. N., Gridley, K. L., Brady, J. N., Phillips, T., and Tyerman, S. D. (2005). The role of molybdenum in agricultural plant production. *Ann. Bot.* 96, 745–754. doi: 10.1093/aob/mci226
- Kerr, S. C., Shafer, M. M., Overdier, J., and Armstrong, D. E. (2008). Hydrologic and biogeochemical controls on trace element export from northern Wisconsin wetlands. *Biogeochemistry* 89, 273–294. doi: 10.1007/s10533-008-9219-2
- King, E. K. (2017). *Understanding Molybdenum Isotope Dynamics in Terrestrial Environments*. Ph.D. thesis, Oregon State University, Corvallis, OR.
- King, E. K., Perakis, S. S., and Pett-Ridge, J. C. (2018). Molybdenum isotope fractionation during adsorption to organic matter. *Geochim. Cosmochim. Acta* 222, 584–598. doi: 10.1016/j.gca.2017.11.014
- King, E. K., Thompson, A., Chadwick, O. A., and Pett-Ridge, J. C. (2016). Molybdenum sources and isotopic composition during early stages of pedogenesis along a basaltic climate transect. *Chem. Geol.* 445, 54–67. doi: 10.1016/j.chemgeo.2016.01.024

- King, E. K., Thompson, A., Hodges, C., and Pett-Ridge, J. C. (2014). Towards understanding temporal and spatial patterns of molybdenum in the critical zone. *Procedia Earth Planet. Sci.* 10, 56–62. doi: 10.1016/j.proeps.2014.08.011
- Kotaš, J., and Stasička, Z. (2000). Chromium occurrence in the environment and methods of its speciation. *Environ. Pollut.* 107, 263–283. doi: 10.1016/S0269-7491(99)00168-2
- Kraepiel, A. M. L., Dere, A. L., Herndon, E. M., and Brantley, S. L. (2015). Natural and anthropogenic processes contributing to metal enrichment in surface soils of central Pennsylvania. *Biogeochemistry* 123, 265–283. doi: 10.1007/s10533-015-0068-5
- Kurtz, A. C., Derry, L. A., Chadwick, O. A., and Alfano, M. J. (2000). Refractory element mobility in volcanic soils. *Geology* 28, 683–686. doi: 10.1130/0091-7613(2000)28<683:REMI>2.0.CO;2
- Larsen, M. C. (2012). “Landslides and sediment budgets in four watersheds in Eastern Puerto Rico,” in *Water Quality and Landscape Processes of Four Watersheds in Eastern Puerto Rico: US Geological Survey Professional Paper*, eds S. F. Murphy and R. F. Stallard (Reston, VA: U.S. Geological Survey), 153–178. doi: 10.3133/pp1789F
- Larsson, M. A., Baken, S., Gustafsson, J. P., Hadialhejazi, G., and Smolders, E. (2013). Vanadium bioavailability and toxicity to soil microorganisms and plants. *Environ. Toxicol. Chem.* 32, 2266–2273. doi: 10.1002/etc.2322
- Larsson, M. A., D’Amato, M., Cubadda, F., Raggi, A., Öborn, I., Kleja, D. B., et al. (2015). Long-term fate and transformations of vanadium in a pine forest soil with added converter lime. *Geoderma* 259, 271–278. doi: 10.1016/j.geoderma.2015.06.012
- Larsson, M. A., Hadialhejazi, G., and Gustafsson, J. P. (2017). Vanadium sorption by mineral soils: development of a predictive model. *Chemosphere* 168, 925–932. doi: 10.1016/j.chemosphere.2016.10.117
- Levina, A., Codd, R., Dillon, C. T., and Lay, P. A. (2003). Chromium in biology: toxicology and nutritional aspects. *Prog. Inorg. Chem.* 51, 145–250.
- Marks, J. A., Perakis, S. S., King, E. K., and Pett-Ridge, J. C. (2015). Soil organic matter regulates molybdenum storage and mobility in forests. *Biogeochemistry* 125, 167–183. doi: 10.1007/s10533-015-0121-4
- Marschner, H., Römheld, V., Horst, W. J., and Martin, P. (1986). Root-induced changes in the rhizosphere: importance for the mineral nutrition of plants. *J. Plant Nutr. Soil Sci.* 149, 441–456. doi: 10.1002/jpln.19861490408
- Martin, H. W., and Kaplan, D. I. (1998). Temporal changes in cadmium, thallium, and vanadium mobility in soil and phytoavailability under field conditions. *Water Air Soil Pollut.* 101, 399–410. doi: 10.1023/A:1004906313547
- Mehra, O. P., and Jackson, M. L. (1960). “Iron oxide removal from soils and clays by a dithionite–citrate system buffered with sodium bicarbonate,” in *Proceedings of the Seventh National Conference on Clays and Clay Minerals*, Washington, DC.
- Morrison, J. M., Goldhaber, M. B., Mills, C. T., Breit, G. N., Hooper, R. L., Holloway, J. M., et al. (2015). Weathering and transport of chromium and nickel from serpentinite in the Coast Range ophiolite to the Sacramento Valley, California, USA. *Appl. Geochem.* 61, 72–86. doi: 10.1016/j.apgeochem.2015.05.018
- Murphy, S. F., Stallard, R. F., Larsen, M. C., and Gould, W. A. (2012). “Physiography, geology, and land cover of four watersheds in eastern Puerto Rico,” in *Water Quality and Landscape Processes of Four Watersheds in Eastern Puerto Rico: US Geological Survey Professional Paper 1789*, eds S. F. Murphy and R. F. Stallard (Reston, VA: U.S. Geological Survey), 1–23.
- Murphy, S. F., Stallard, R. F., Scholl, M. A., González, G., and Torres-Sánchez, A. J. (2017). Reassessing rainfall in the Luquillo Mountains, Puerto Rico: local and global ecohydrological implications. *PLoS One* 12:e0180987. doi: 10.1371/journal.pone.0180987
- Orlando, J., Comas, X., Hynek, S. A., Buss, H. L., and Brantley, S. L. (2016). Architecture of the deep critical zone in the Rio Icacos watershed (Luquillo critical zone observatory, Puerto Rico) inferred from drilling and ground penetrating radar (GPR). *Earth Surf. Process. Landf.* 41, 1826–1840. doi: 10.1002/esp.3948
- Pearce, C. R., Burton, K. W., Pogge von Strandmann, P. A. E., James, R. H., and Gíslason, S. R. (2010). Molybdenum isotope behaviour accompanying weathering and riverine transport in a basaltic terrain. *Earth Planet. Sci. Lett.* 295, 104–114. doi: 10.1016/j.epsl.2010.03.032
- Pérez, C., Antelo, J., Fiol, S., and Arce, F. (2014). Modeling oxyanion adsorption on ferralic soil, part 2: chromate, selenate, molybdate, and arsenate adsorption. *Environ. Toxicol. Chem.* 33, 2217–2224. doi: 10.1002/etc.2581
- Pett-Ridge, J. C., Derry, L. A., and Barrows, J. K. (2009). Ca/Sr and 87Sr/86Sr ratios as tracers of Ca and Sr cycling in the Rio Icacos watershed, Luquillo Mountains, Puerto Rico. *Chem. Geol.* 267, 32–45. doi: 10.1016/j.chemgeo.2008.11.022
- Pokrovsky, O. S., and Schott, J. (2002). Iron colloids/organic matter associated transport of major and trace elements in small boreal rivers and their estuaries (NW Russia). *Chem. Geol.* 190, 141–179. doi: 10.1016/S0009-2541(02)00115-8
- Prouty, N. G., Swarzenski, P. W., Fackrell, J. K., Johannesson, K., and Palmore, C. D. (2017). Groundwater-derived nutrient and trace element transport to a nearshore Kona coral ecosystem: experimental mixing model results. *J. Hydrol. Reg. Stud.* 11, 166–177. doi: 10.1016/j.ejrh.2015.12.058
- Richter, D. D. Jr., and Markewitz, D. (2001). *Understanding Soil Change: Soil Sustainability Over Millennia, Centuries, and Decades*. New York, NY: Cambridge University Press.
- Riley, M. M., Robson, A. D., Gartrell, J. W., and Jeffery, R. C. (1987). The absence of leaching of molybdenum in acidic soils from Western Australia. *Soil Res.* 25, 179–184. doi: 10.1071/SR9870179
- Salvador-Blanes, S., Cornu, S., Bourennane, H., and King, D. (2006). Controls of the spatial variability of Cr concentration in topsoils of a central French landscape. *Geoderma* 132, 143–157. doi: 10.1016/j.geoderma.2005.05.003
- Saputro, S., Yoshimura, K., Matsuoka, S., Takehara, K., Narsito, A. J., and Tennichi, Y. (2014). Speciation of dissolved chromium and the mechanisms controlling its concentration in natural water. *Chem. Geol.* 364, 33–41. doi: 10.1016/j.chemgeo.2013.11.024
- Schwertmann, U., and Pfab, G. (1996). Structural vanadium and chromium in lateritic iron oxides: genetic implications. *Geochim. Cosmochim. Acta* 60, 4279–4283. doi: 10.1016/S0016-7037(96)00259-1
- Shiller, A. M. (1997). Dissolved trace elements in the Mississippi River: seasonal, interannual, and decadal variability. *Geochim. Cosmochim. Acta* 61, 4321–4330. doi: 10.1016/S0016-7037(97)00245-7
- Shiller, A. M., and Boyle, E. A. (1987). Dissolved vanadium in rivers and estuaries. *Earth Planet. Sci. Lett.* 86, 214–224. doi: 10.1016/0012-821X(87)90222-6
- Shiller, A. M., and Mao, L. (2000). Dissolved vanadium in rivers: effects of silicate weathering. *Chem. Geol.* 165, 13–22. doi: 10.1016/S0009-2541(99)00160-6
- Siebert, C., Pett-Ridge, J. C., Opfergelt, S., Guicharnaud, R. A., Halliday, A. N., and Burton, K. W. (2015). Molybdenum isotope fractionation in soils: influence of redox conditions, organic matter, and atmospheric inputs. *Geochim. Cosmochim. Acta* 162, 1–24. doi: 10.1016/j.gca.2015.04.007
- Singh, H. P., Mahajan, P., Kaur, S., Batish, D. R., and Kohli, R. K. (2013). Chromium toxicity and tolerance in plants. *Environ. Chem. Lett.* 11, 229–254. doi: 10.1007/s10311-013-0407-5
- Solé, V. A., Papillon, E., Cotte, M., Walter, P., and Susini, J. (2007). A multiplatform code for the analysis of energy-dispersive X-ray fluorescence spectra. *Spectrochim. Acta Part B* 62, 63–68. doi: 10.1016/j.sab.2006.12.002
- Strady, E., Blanc, G., Schäfer, J., Coynel, A., and Dabrin, A. (2009). Dissolved uranium, vanadium and molybdenum behaviours during contrasting freshwater discharges in the Gironde Estuary (SW France). *Estuar. Coast. Shelf Sci.* 83, 550–560. doi: 10.1016/j.eccs.2009.05.006
- Tian, Z. (2018). *Soil and Weathered Bedrock Evolution Along an Elevation Gradient in the Southern Sierra Nevada, California*. Doctoral dissertation, University of California, Davis.
- Trostle, K. D., Ray Runyon, J., Pohlmann, M. A., Redfield, S. E., Pelletier, J., McIntosh, J., et al. (2016). Colloids and organic matter complexation control trace metal concentration-discharge relationships in Marshall Gulch stream waters. *Water Resour. Res.* 52, 7931–7944. doi: 10.1002/2016WR019072
- Weaver, P. L., and Gould, W. A. (2013). “Forest vegetation along environmental gradients in northeastern Puerto Rico,” in *Ecological Gradient Analyses in a Tropical Landscape*, Vol. 54, eds G. González, M. R. Willig, and R. B. Waide (Oxford: John Wiley & Sons), 43–66.
- White, A. F., Blum, A. E., Schulz, M. S., Vivit, D. V., Stonestrom, D. A., Larsen, M., et al. (1998). Chemical weathering in a tropical watershed, Luquillo Mountains, Puerto Rico: I. Long-term versus short-term weathering fluxes. *Geochim. Cosmochim. Acta* 62, 209–226. doi: 10.1016/S0016-7037(97)00335-9

- Wichard, T., Mishra, B., Myneni, S. C., Bellenger, J. P., and Kraepiel, A. M. (2009). Storage and bioavailability of molybdenum in soils increased by organic matter complexation. *Nat. Geosci.* 2, 625–629. doi: 10.1038/ngeo589
- Wisawapipat, W., and Kretzschmar, R. (2017). Solid phase speciation and solubility of vanadium in highly weathered soils. *Environ. Sci. Technol.* 51, 8254–8262. doi: 10.1021/acs.est.7b01005
- Xu, N. A. N., Braida, W., Christodoulatos, C., and Chen, J. (2013). A review of molybdenum adsorption in soils/bed sediments: speciation, mechanism, and model applications. *Soil Sediment Contam.* 22, 912–929. doi: 10.1080/15320383.2013.770438

Conflict of Interest Statement: The authors declare that the research was conducted in the absence of any commercial or financial relationships that could be construed as a potential conflict of interest.

Copyright © 2018 Richardson and King. This is an open-access article distributed under the terms of the Creative Commons Attribution License (CC BY). The use, distribution or reproduction in other forums is permitted, provided the original author(s) and the copyright owner(s) are credited and that the original publication in this journal is cited, in accordance with accepted academic practice. No use, distribution or reproduction is permitted which does not comply with these terms.